Mat. Res. Soc. Symp. Proc. Vol. 674 © 2001 Materials Research Society

Effect of Composition and Processing on the Microstructure and Magnetic Properties of 2:17 High Temperature Magnets

W. Tang, Y. Zhang, D. Goll[1], H. Kronmüller[1] and G. C. Hadjipanayis
University of Delaware, Dept. of Physics & Astronomy, Newark, DE 19716, USA
[1]Max-Planck Institut für Metallforschung, D-70569 Stuttgart, Germany

ABSTRACT

A comprehensive and systematic study has been made on $Sm(Co_{bal}Fe_vCu_yZr_x)_z$ magnets to completely understand the effects of composition and processing on their magnetic properties. The homogenized $Sm(Co,Fe,Cu,Zr)_z$ magnets have a featureless microstructure. A cellular/lamellar microstructure develops after 2-3 hours of aging at 800-850°C, but the coercivity increases only after a subsequent slow cooling to 400°C. During cooling, diffusion takes place and Cu is concentrated in the 1:5 cell boundaries and Fe in the 2:17R cells. This dilutes the magnetic properties of the 1:5 phase and causes domain wall pinning/nucleation at the cell boundaries. Higher ratio z leads to larger cells as expected due to the larger amount of the 2:17 phase. For a fixed Cu content, this translates to a larger amount of Cu in the 1:5 cell boundaries, and therefore, to a higher coercivity. Magnets without Cu but with Zr have a lamellar and a cellular like microstructure. In Zr free samples, however, a larger amount of Cu is needed to form the cellular microstructure. This cellular microstructure is unstable with prolonged isothermal aging. A uniform and stable cellular/lamellar microstructure is only observed in alloys containing both Cu and Zr. A higher aging temperature T_{ag} leads to larger cells and higher coercivity as explained above. The results of all these studies clearly show that the amount of Cu in the 1:5 cell boundaries controls both the coercivity and its temperature dependence leading to positive and negative temperature coefficients of coercivity in low and high Cu content alloys, respectively.

INTRODUCTION

$Sm(Co,Fe,Cu,Zr)_z$ permanent magnets are characterized by large anisotropy fields and high Curie temperatures which make them suitable candidates for high temperature applications [1, 2]. The optimum properties of the magnets are obtained after a lengthy heat treatment consisting of homogenization at a temperature T_h (1160-1190°C), slightly below the sintering temperature, followed by an aging at temperatures T_{ag} between 800-850°C, and a subsequent slow cooling to 400°C. Their high coercivity originates from a complex microstructure consisting of a superposition of cellular (2:17 cells and 1:5 cell boundaries) with a lamellar structure known as the Z phase. Cu is found to be concentrated in the 1:5 cell boundaries and Zr in the Z phase. According to Ray [3], Cu stabilizes the $Sm(Co, Cu)_5$ phase in the presence of Fe and Fe stabilizes the 2:17R phase in the presence of Cu. The $Sm_2(Co,Fe)_{17}$ cells are mainly responsible for the large saturation magnetization while the $Sm(Co, Cu)_5$ cell boundaries pin the domain-walls [4]. Lorentz microscopy studies [5, 6] clearly showed wavy domain walls following the 1:5 cell boundaries, indicating domain wall pinning at the latter. The Zr-rich lamella phase is believed to provide diffusion paths for Cu segregation and thus to form uniform $Sm(Co,Cu)_5$ cell boundary phase, which leads to high coercivity [7].

The $Sm(Co_{bal}Fe_vCu_yZr_x)_z$ magnets represent a complex system with four compositional variables (x, y, v, z) and five heat treating variables (T_h, t_h, T_{ag}, t_{ag}, dT/dt). We have recently undertaken a comprehensive and systematic study (MURI Project) on cast alloys and sintered magnets to understand the effects of composition (z, x, y, v) and processing on their magnetic hardening behavior, particularly on H_{ci} and its temperature dependence. These studies led to the development of new high temperature magnets with controlled temperature dependence of H_{ci} (including an abnormal temperature dependence of coercivity $H_c(T)$ in some magnets) [8-10] having a record value of 10 kOe at 500°C [11]. From these studies, we are able to finely tune the microstructure and microchemistry of the Sm-Co magnets through adjustments in the composition and processing parameters, and design magnets for various applications. In addition, the discovery of the abnormal temperature behavior has posed a new challenge about how to explain their magnetization reversal mechanism. This paper summarizes our studies on the effect of composition and processing on the microstructure and magnetic properties, and discuss the magnetization reversal mechanism with respect to the $H_c(T)$ of $Sm(Co_{bal}Fe_vCu_yZr_x)_z$ magnets.

EXPERIMENTAL PROCEDURES

Cast samples with nominal composition $Sm(Co_{bal}Fe_vCu_yZr_x)_z$ with x=0-0.1, y=0.048-0.168, v=0-0.3 and z=7.0-9.0 were prepared by arc-melting. All the samples were solutionized (homogenized) at 1170-1190°C. The aging heat treatments were carried at temperatures in the range of 700-900°C. The isothermal aging time was varied from 0.5 to 24h. After isothermal aging, the samples were subjected to either a quenching to room temperature or to a slow cooling to 400°C. In addition, some samples were cooled to intermediate temperatures and then quenched to room temperature. The room temperature magnetic properties were measured using an Oxford vibrating sample magnetometer (VSM) with a maximum applied field of 5 T. The high temperature magnetic properties were measured using a high temperature VSM with an applied field of 20 kOe. Microstructure analysis was carried out using a JEOL JEM-2000 FX transmission electron microscope (TEM). Nanoprobe chemical analysis was carried out using JEOL 2010 FEG with 1nm resolution.

RESULTS AND DISCUSSION

Compositions required for the formation of cellular/lamellar microstructure

Binary Sm-Co alloys with composition close to that of 2:17 magnets do not show the cellar/lamellar microstructure. Figure 1 shows the microstructure of the stoichiometric $Sm_{11}Co_{89}$ and $Sm_{14}Co_{86}$ samples without Cu and Zr addition. The microstructure of $Sm_{11}Co_{89}$ sample mainly consists of the 2:17 phase with many dislocations present [see Fig. 1 (a)]. With increasing Sm content (i. e. decreasing ratio z) in the alloys, a certain amount of 1:5 phase is observed besides the 2:17 phase as seen in Fig. 1(b). However, the cellular microstructure is not yet formed. When x=2.5 at.% Zr is added, the lamellar structure is observed with an incomplete cellular microstructure (see Fig. 2). However, the coercivity of the sample is almost zero due to the lack of a large gradient in domain wall energy across the 1:5 boundaries. In Zr free

$Sm(Co_{bal}Fe_{0.1}Cu_y)_{8.5}$ magnets with y=0.088, the cellular/lamellar microstructure is not formed. A rod or needle-like 1:5 phase is distributed in the 2:17 matrix instead (Fig. 3a). If the Cu content y is increased to 0.168, a very fine (35 nm) cellular microstructure is formed with a maximum H_{ci}=5.6 kOe after aging (Fig. 3b). However, the cell size cannot be uniformly grown and finally breaks down with further aging [9]. As it will be seen later, in order to obtain a high coercivity, a uniform cellular and lamellar microstructure is required and this is the result when both Cu and Zr are present in Sm-Co alloys.

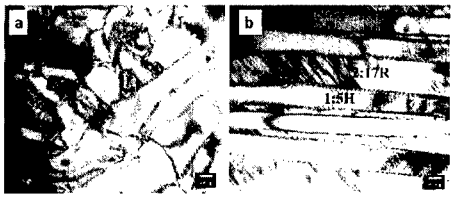

Figure 1. TEM micrographs of $Sm_{11}Co_{89}$ (a) and $Sm_{14}Co_{86}$ (b) samples.

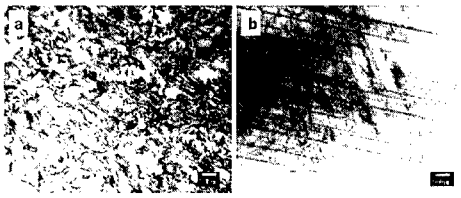

Figure 2. TEM micrographs of a $Sm_{11}Co_{86.5}Zr_{2.5}$ sample. (a) perpendicular, and (b) parallel to the c-axis of the 2:17 phase

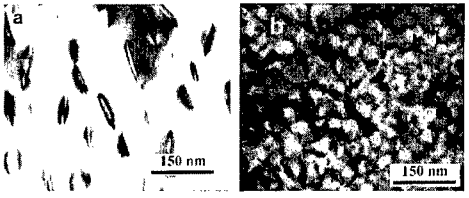

Figure 3. The TEM cellular microstructures for the $Sm(Co_{bal}Fe_{0.1}Cu_y)_{8.5}$ magnets with (a) y=0.088 and (b) 0.168, respectively.

Effect of ratio z

Ratio z defines the ratio of TTM/Sm (TTM=total transition metal). According to the phase diagram [12], magnets with a low ratio z (i.e. high Sm content) would be expected to have more of the $Sm(Co,Cu)_5$ cell boundary phase. Figure 4 shows the cellular microstructure of $Sm(Co_{bal}Fe_{0.224}Cu_{0.08}Zr_{0.033})_z$ magnets with z=7.0, 8.5 and 9.1 obtained by TEM (magnets with z>8.5 have a small amount of Co present). It is clear that when the ratio z increases from 7.0 to

8.5 and 9.0, the average cell size increases to 88, 108 and 237 nm, respectively. For a fixed Cu content, a larger cell size results in a larger amount of Cu in the 1:5 cell boundaries. This leads to a larger gradient in domain wall energy across the cell boundaries resulting in a stronger domain wall pinning, and gives rise to a higher coercivity. For high z the cellular microstructure is not complete and the coercivity deteriorates. Figure 5 shows the temperature dependence of intrinsic coercivity of $Sm(Co_{bal}Fe_{0.1}Cu_{0.088}Zr_{0.04})_z$ magnets with different ratio z. It is seen that the magnets with lower z have better $H_c(T)$. In addition, an abnormal $H_c(T)$ is observed in the magnets with z=7.0. Both of these effects will be discussed later.

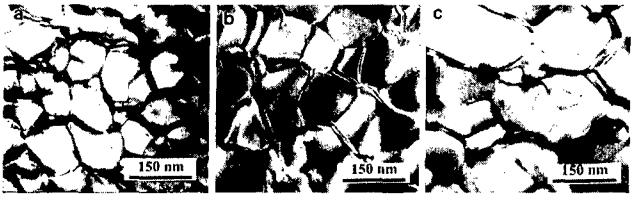

Figure 4. The cellular microstructure of $Sm(Co_{bal}Fe_{0.224}Cu_{0.08}Zr_{0.033})_z$ magnets with (a) z=7.0, H_{ci}=15 kOe, (b) z=8.5, H_{ci}=35 kOe and z=9.1, H_{ci}=8 kOe.

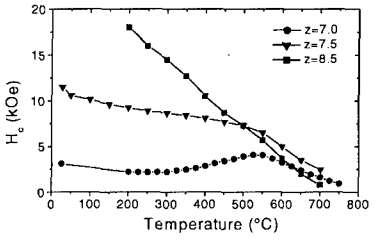

Figure 5. The temperature dependence of intrinsic coercivity H_{ci} of $Sm(Co_{bal}Fe_{0.1}Cu_{0.088}Zr_{0.04})_z$ magnets with different ratio z.

Effect of Cu

Cu content has the most important effect on the microstructure and magnetic properties of the magnets. Figure 6 shows the dependence of intrinsic coercivity H_{ci} and saturation magnetization M_s of $Sm(Co_{bal}Fe_{0.1}Cu_yZr_{0.04})_z$ magnets (y=0.048-0.168, z=7.5 and 8.5) on the Cu content. M_s decreases while H_{ci} increases with increasing Cu content. It is noted that the H_{ci} of the magnets with z=8.5 reaches a maximum of about 40 kOe when the Cu content x is 0.088. However, for the magnets with z=7.5, H_{ci} continues to increase with increasing the Cu content y up to 0.168. The TEM microstructure of $Sm(Co_{bal}Fe_{0.1}Cu_yZr_{0.04})_z$ magnets [11] shows that the cell size decreases slightly with increasing Cu content with a stronger dependence in the case of high ratio z. The average cell size decreases from 120 to 75 nm with increasing the Cu content from 0.048 to 0.168. Our nanoprobe chemical analysis results (see Fig. 16 in the section of magnetic hardening) show that Cu is concentrated at the cell boundaries and Cu content increases with increasing the Cu content of the magnets. Because the magnet with low ratio z has a smaller

cell size, the proportion of the cell boundaries is larger. More Cu is needed to obtain a large domain wall gradient across the cell boundaries. Even when the Cu content is up to 0.168, the coercivity has not yet reached its maximum. The temperature dependence of $Sm(Co_{bal}Fe_{0.1}Cu_yZr_{0.04})_{7.5}$ magnets with different Cu content y is shown in Fig. 7. The magnets with lower Cu content have lower room temperature coercivity but exhibit a better $H_c(T)$.

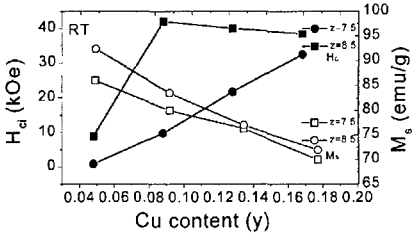

Figure 6. The dependence of saturation magnetization M_s and intrinsic coercivity H_{ci} on the Cu content in $Sm(Co_{bal}Fe_{0.1}Cu_yZr_{0.04})_z$ magnets (y=0.048-0.168, z=7.5 and 8.5).

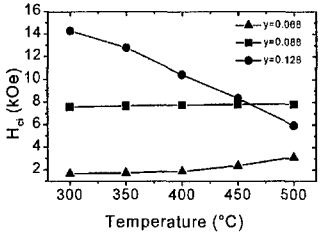

Figure 7. The temperature dependence of intrinsic coercivity H_{ci} of $Sm(Co_{bal}Fe_{0.1}Cu_yZr_{0.04})_{7.5}$ magnets with different Cu content.

Effect of Zr

Although many studies in the past have examined the role of Zr [3, 7, 13, 14], yet its effect is not fully understood. Figure 8 shows the optimized intrinsic coercivity H_{ci} as a function of Zr content in $Sm(Co_{bal}Fe_{0.1}Cu_{0.088}Zr_x)_{8.5}$ magnets at 25 and 500°C, respectively. At room temperature, the coercivity is below 2 kOe for the sample without Zr. However, with increasing Zr content, the coercivity dramatically increases and reaches a value of around 40 kOe for x in the range from 0.015 to 0.06. When x>0.06, the coercivity begins to decrease. At 500°C, although the coercivity is below 10 kOe for all magnets, it still gradually increases with increasing x up to 0.06 and then it decreases significantly.

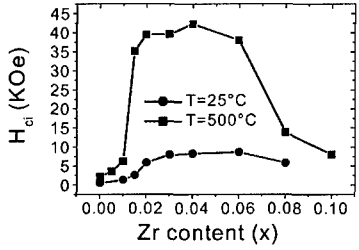

Figure 8. Effect of Zr on the coercivity of $Sm(Co_{bal}Fe_{0.1}Cu_{0.088}Zr_x)_{8.5}$ magnets at 25 and 500°C

Figure 9 shows TEM cellular microstructures for the $Sm(Co_{bal}Fe_{0.1}Cu_{0.088}Zr_x)_{8.5}$ magnets with (a) x=0.005, (b) 0.04 and (c) 0.08, respectively. With increasing x from 0 to 0.08, the microstructure gradually changes from the 2:17 matrix along with a needle-like 1:5 phase [Fig. 3(a)] to an incomplete cellular [Fig. 9(a)], and finally a uniform cellular, while the cell size decreases, first slightly and then quickly, from 120 to 35 nm. On the other hand, the density of lamella phase increases, first quickly and then slightly, from 0.024 to 0.062 nm^{-1} [15, 16]. When the Zr content is further increased to over 0.08, a 2:7 phase is formed leading to a decrease in coercivity [17].

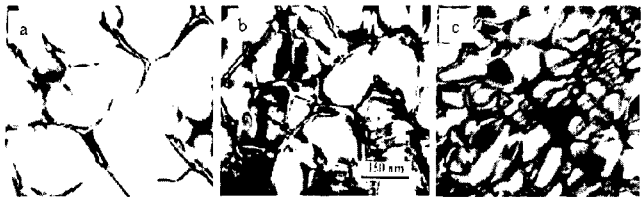

Figure 9. The TEM cellular microstructures for the $Sm(Co_{bal}Fe_{0.1}Cu_{0.088}Zr_x)_{8.5}$ magnets with (a) x=0.005, (b) 0.04 and (c) 0.08, respectively.

Figure 10 shows the effect of isothermal aging time on the coercivity of $Sm(Co_{bal}Fe_{0.1}Cu_{0.088}Zr_x)_{8.5}$ magnets with different Zr content. Because Zr helps the redistribution of Cu at the cell boundaries, the development of high coercivity with the isothermal aging time strongly depends on the Zr content in magnets.

As mentioned before in Zr-free magnets with higher Cu content, a fine cellular microstructure is observed which becomes highly non-uniform with aging. After the addition of Zr and Cu in the magnets, a normal microstructure consisting of rhombohedral $Sm_2(Co,Fe)_{17}$ cells surrounded by a Cu-rich hexagonal $Sm(Co,Cu)_5$ cell boundary phase is always formed. These results indicate that the lamellar phase formed by adding Zr stabilizes a uniform cellular microstructure with the right microchemistry for high coercivity [9].

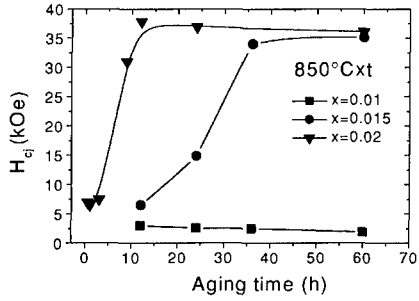

Figure 10. The coercivity as a function of aging time for $Sm(Co_{bal}Fe_{0.1}Cu_{0.088}Zr_x)_{8.5}$ magnets with different Zr content.

Effect of Fe

Iron has a significant effect on the high temperature magnetic properties of $Sm(Co,Fe,Cu,Zr)_z$ magnets. Some studies [17, 18] suggested that the high temperature performance of SmCo 2:17 magnets can be improved by decreasing the Fe content. Our results show that for some compositions the addition of a certain amount of Fe is necessary to develop a uniform cellular microstructure with a larger cell size and thus a high coercivity. The TEM studies for $Sm(Co_{bal}Fe_vCu_{0.128}Zr_{0.02})_{7.0}$ magnets with different v (see Fig. 11) show that the magnet with low Fe content has a smaller but non-uniform cell size (The average cell size is 48 nm). With increasing the Fe content v up to 0.2, the cell size increases to 120 nm but becomes uniform because Fe substitutes in the 2:17 phase. As explained earlier, for a fixed Cu, this leads to a larger Cu content in the 1:5 cell boundaries and therefore, to a higher coercivity. When the Fe content is further increased up to 0.25, the cell size continuously increases up to 180 nm and becomes inhomogeneous. The cellular structure starts deteriorating and this leads to the decrease of coercivity. In the $Sm(Co_{bal}Fe_vCu_{0.078}Zr_{0.033})_{8.3}$ magnet with higher ratio z [19], because the original cell size is large, the addition of Fe does not have a significant effect on the microstructure and coercivity.

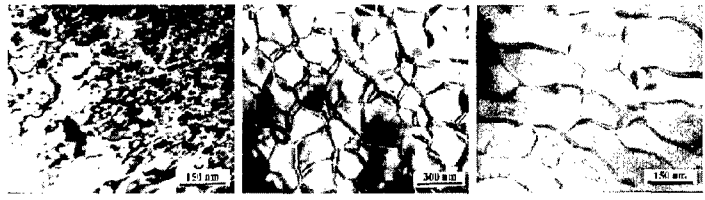

Figure 11: TEM micrographs of $Sm(Co_{bal}Fe_vCu_{0.128}Zr_{0.02})_{7.0}$ magnets (a) v=0, (b) v=0.02 and (c) v=0.25.

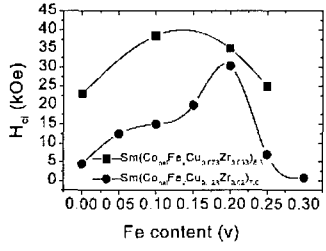

Figure 12. The effect of Fe content on the intrinsic coercivity H_{ci} of magnets with different compositions.

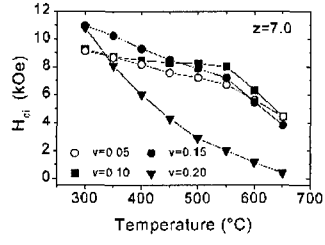

Figure 13. The temperature dependence of intrinsic coercivity H_{ci} of $Sm(Co_{bal}Fe_{0.1}Cu_{0.128}Zr_{0.02})_{7.0}$ magnets with different Fe.

Figure 12 shows the effect of Fe content on the magnetic properties of magnets with different compositions. Although a maximum of coercivity exists with Fe content, the coercivity of $Sm(Co_{bal}Fe_yCu_{0.128}Zr_{0.02})_{7.0}$ magnet with a low ratio z is more sensitive to the Fe content. More Fe is needed to develop a high coercivity. The $H_c(T)$ of $Sm(Co_{bal}Fe_yCu_{0.128}Zr_{0.02})_{7.0}$ magnets with different Fe content (see Fig. 13) show that the coercivity of all magnets always decreases with increasing temperature. However, the $H_{ci}(T)$ curves for the magnets with higher Fe content are steeper. This is probably due to the lower anisotropy K of the 2:17 matrix phase and its stronger temperature dependence $K(T)$, because of the lower Curie temperature of the 2:17 matrix phase.

Effect of aging temperature and time

Figure 14 shows the dependence of coercivity H_{ci} on the aging temperature T_{ag} in a $Sm(Co_{bal}Fe_{0.1}Cu_{0.088}Zr_{0.04})_{8.5}$ magnet. It can be seen that the magnet aged at 850°C has an optimal coercivity. The TEM image shows that the magnet aged at 750°C has a smaller cell size (70 nm). Additional data about the microstructure and coercivity of sintered $Sm(Co,Fe,Cu,Zr)_{6.4}$ magnets with different aging temperature is listed in Table 1. Although the Cu concentration at the cell boundaries is almost the same with different aging temperature, the difference of microstructure parameters, especially the thickness of cell boundaries, results in a different coercivity. A higher T_{ag} leads to larger cells and thicker cell boundaries and thus leads to higher coercivity. It is reasonable to assume that an increase of T_{ag} over 850°C leads to a further increase and final deterioration of the cell size, and thus it leads to a reduction in coercivity.

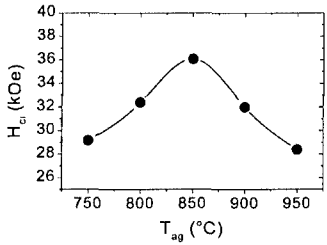

Figure 14: Dependence of coercivity H_{ci} on the aging temperature T_{ag} in a $Sm(Co_{bal}Fe_{0.1}Cu_{0.088}Zr_{0.04})_{8.5}$ magnet.

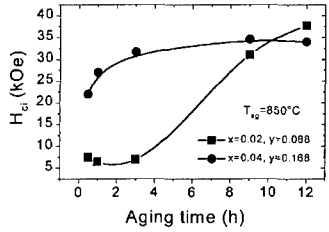

Figure 15. The dependence of intrinsic coercivity H_{ci} on the aging time for $Sm(Co_{bal}Fe_{0.1}Cu_yZr_x)_{8.5}$ magnets with different Cu and Zr content.

Figure 15 shows the dependence of coercivity on the aging time for $Sm(Co_{bal}Fe_{0.1}Cu_yZr_x)_{8.5}$ magnets with different Cu and Zr content. For the magnet with low Cu and Zr content, an optimal coercivity is developed only after aging at 850°C for over 9h, followed by the slow cooling. However, the development of coercivity for the $Sm(Co_{bal}Fe_{0.1}Cu_{0.168}Zr_{0.04})_{8.5}$ magnet is not sensitive to the isothermal aging time at 850°C. The magnet develops a coercivity of over 21 kOe even after aging at 850°C for 0.5h, followed by a slow cooling to 400°C. This suggests that higher Cu content along with a certain amount of Zr permits the rapid formation of the right microstructure and microchemistry during aging and thus it leads to the observed high coercivity [10]. These results are also consistent with the studies on the evolution of microstructure and nanoscale composition [21], which shows that a perfect cellular/lamellar microstructure is formed

after aging for 2h at 850°C, while Cu diffusion at the cell boundaries mainly occurs during a slow cooling stage.

Table I. Effect of aging temperature on the microstructure parameters and coercivity of a sintered $Sm(Co,Fe,Cu,Zr)_{6.4}$ magnet.

T_{ag} (°C)	H_{ci} (kOe)	Cell size (nm)	Boundary width (nm)	Density of lamella (nm)	Cu content in cell boundary (nm)
700	6.5	50	6.5	0.046	14.4
800	13	105	11	0.061	15.7

Magnetic hardening

Recently our extensive studies show that the distribution and amount of Cu at the 1:5 cell boundaries is the predominant factor in controlling the pinning strength or magnetization reversal and therefore the coercivity and its temperature dependence. Figure 16 shows a typical element profile along the cell boundary obtained by nanoprobe chemical analysis for the $Sm(Co_{bal}Fe_{0.1}Cu_{0.128}Zr_{0.02})_{7.5}$ magnet. Cu mainly concentrates at the 1:5 cell boundaries and increases from 13.8 to 33.8 at. % with Cu increasing from 0.068 to 0.128.

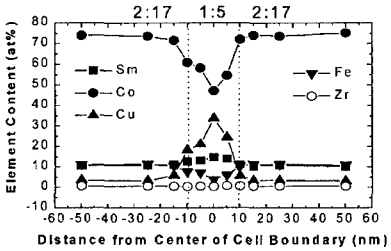

Figure 16. An element profile along the cell boundary for $Sm(Co_{bal}Fe_{0.1}Cu_{0.128}Zr_{0.02})_{7.5}$ magnet.

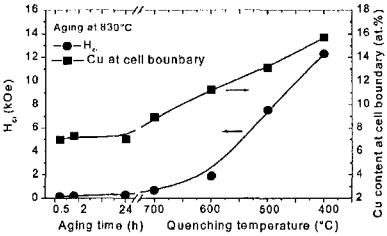

Figure 17: The evolution of Cu at cell boundaries and coercivity with heat treatment.

Figure 17 shows the evolution of Cu at the cell boundaries and coercivity with heat treatment. It can be seen that the development of coercivity closely follows the changes of Cu content at the cell boundaries. A large Cu gradient at the cell boundaries is obtained by the low temperature slow cooling close to 400°C, which then leads to large coercivities. These results further confirm that the Cu content plays an important role in the development of coercivity. In addition, the $H_c(T)$ study on Cu-free $Sm_{11}Co_{86.5}Zr_{2.5}$ sample shows that an abnormal $H_c(T)$ exits, and is reversible with temperature. Because the sample is Cu-free, the abnormal $H_c(T)$ should be caused due to the presence of cellular microstructure. Therefore, the abnormal $H_C(T)$ is related to both the presence of cellular microstructure and distribution of Cu at cell boundaries.

Figure 18 show the $H_C(T)$ for $Sm(Co_{bal}Fe_{0.1}Cu_yZr_{0.04})_{7.0}$ magnets with different Cu content. These magnets have the cellular/lamellar structure. It can be seen that the room temperature coercivity increases with increasing Cu content. The abnormal $H_C(T)$ is observed in the magnets with lower Cu content. Additionally, it is noted that the temperature of the peak coercivity at high temperature decreases with increasing Cu content. Figure 19 shows the temperature dependence

of anisotropy constant K_1 for some 1:5 and 2:17 compounds (after [22-24]). Because Cu mainly goes into the 1:5 boundary phase, it is assumed the K_1 of 2:17 phase remains constant with increasing Cu content. It has been shown that the K_1 of the 1:5 phase gradually decreases with increasing Cu content, leading to the gradual reduction of the critical temperature T_{cr} , where K_1 (1:5)=K_1 (2:17). The abnormal H_c(T) behavior can be explained by using both the pinning and nucleation models.

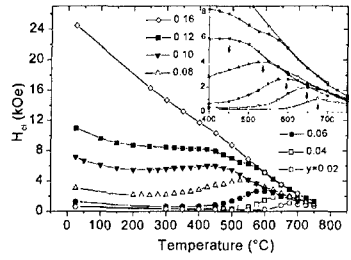

Figure 18. Temperature dependence of coercivity for $Sm(Co_{bal}Fe_{0.1}Cu_yZr_{0.04})_{7.0}$ magnets with different Cu content.

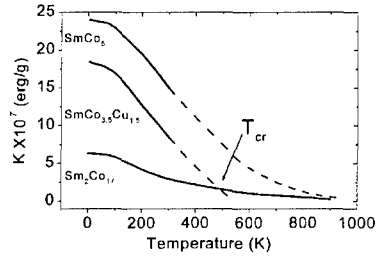

Figure 19. Temperature dependence of anisotropy K for 1:5 and 2:17 compounds [22-24].

According to the two-phase pinning mechanism [25], the coercivity is proportional to the $\Delta\gamma$ between the domain-wall energies $\gamma=4(AK_1)^{0.5}$ for the two phases, where $\Delta\gamma=\gamma_{2:17}-\gamma_{1:5}$, A is the exchange stiffness. If the Cu content is low, below a critical temperature T_{cr}, the γ(1:5) is higher than γ(2:17) leading to a relatively weak repulsive pinning. Above T_{cr}, the γ(1:5) is lower than γ (2:17) leading to an attractive pinning with an increase in coercivity. Moreover, with increasing Cu content, T_{cr} moves in the direction of low temperature, which leads to the shift of peak coercivity to lower temperature (see Fig. 18). If the Cu content is sufficiently high, the γ(1:5) is lower than γ(2:17) at any temperature range. Therefore, the abnormal H_C(T) disappears and the coercivity monotonically decreases with increasing temperature. However, this model predicts a minimum value of coercivity at T_{cr} (There may be a distribution of T_{cr} due to the inhomogeneous microchemistry at cell boundaries.). This, however, could not be observed in our experimental data. Our results show that the abnormal H_c(T) behavior is observed in magnets with a wide range of Cu content (0-0.12). These results suggest that the coercivity is controlled by

magnetization reversal in magnetically isolated 2:17 cells at $T_c(1:5)<T<T_c(2:17)$, where T_c is the Curie temperature.

In the Sm-Co magnets, each 2:17 cell is partially or totally surrounded by the 1:5 boundary phase. In this case, the coercivity and its temperature dependence are mainly determined by the anisotropy of the 2:17 phase and its temperature dependence. The 1:5 cell boundary controls the strength of magnetization reversal nucleation with different Cu content or temperature. Figure 20 shows a schematic representation of a single cell under different conditions. When the Cu content is very low, the 2:17 cells are not entirely surrounded by 1:5 boundaries and thus are not completely isolated by the 1:5 cell boundaries [Fig.20(a)], leading to a low coercivity. With increasing Cu content, a uniform cellular microstructure is observed and the 1:5 boundary becomes close to nonmagnetic, resulting in complete magnetic isolation of the 2:17 cells [Fig. 20(b)] and thus a high room temperature coercivity. On the other hand, the magnetic transformation of the 1:5 boundaries caused by increasing temperature is similar to that by increasing Cu content. At $T>T_c$ (1:5), the 2:17 cells are completely isolated and this results in an increase of coercivity. Because the increase of Cu content leads to the reduction of T_c (1:5), the temperature of the peak coercivity at high temperature decreases with increasing Cu content (see Fig. 18). After the 2:17 phase has been isolated at room temperature, the abnormal behavior disappears and the coercivity monotonically decreases with increasing temperature because of thermal activation and $K(T)$ dependence.

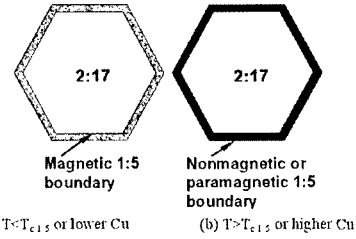

Figure 20. Schematic representation of the 1:5 cell boundaries under different conditions.

CONCLUSIONS

The coercivity and its temperature dependence in $Sm(Co_{bal}Fe_vCu_yZr_x)_z$ magnets are very sensitive to the composition and processing parameters, which in turn affect the microstructure and microchemistry of the magnets. All of these effects lead to a change of the cell size, which in turn leads to a variation of the amount of Cu concentration in the $Sm(Co,Cu)_5$ cell boundaries. The distribution and amount of Cu at the 1:5 cell boundaries is the predominant factor in controlling the magnetization reversal and therefore the coercivity and its temperature dependence. The addition of Zr stabilizes a uniform cellular microstructure with the right microchemistry for high coercivity. The addition of a certain amount of Fe is necessary to develop a uniform cellular microstructure with a larger cell size and thus a high coercivity. The isothermal aging temperature and time mainly change the microstructure parameters, including the cell size, boundary thickness, and density of lamella. The increase of the Cu and Zr content assists in the development of the right microstructure and microchemistry with high coercivity. The temperature dependence of coercivity of magnets with different Cu content cannot be

completely explained by the traditional domain-wall pinning models based on the difference in domain wall energy between the Cu substituted 1:5 and the 2:17 phases. The coercivity and its temperature dependence may also be explained by the nucleation of reversed domains in magnetically isolated Sm_2Co_{17} cells.

ACKNOWLEDGEMENTS

The authors gratefully acknowledge the support of the Air Force Office of Scientific Research (AFOSR) under the "MURI 96" program, award #F49620-96-0434. The authors would also like to thank Dr. J. F. Liu for his contributions on this work.

REFERENCES

1. A. E. Ray and S. Liu, *J. Mater. Eng. Perform,* **1**, 183(1992).
2. G. C. Hadjipanayis, in *Rare earth iron permanent magnets*, edited by J. M. D. Coey (Oxford University Press, Inc., New York, 1996).
3. A. E. Ray, *J. Appl. Phys.*, **55**, 2094(1984).
4. K. Kumar, *J. Appl. Phys.*, **63**, R13(1988).
5. J. Fidler and P. Skalicky, *J. Magn. Magn. Mater.*, **30**, 58(1982).
6. R. K. Mishra, G. Thomas, T. Yoneyama, A. Fukino, and T. Ojima, *J. Appl. Phys.***52**, 2517(1981).
7. L. Rabenberg, R. K. Mishra, and G. Thomas, *J. Appl. Phys.*, **53**, 2389(1982).
8. J. F. Liu, T. Chui, D. Dimitar, and G. C. Hadjipanayis, *Appl. Phys. Lett.* **73**, 3007(1998).
9. W. Tang, Y. Zhang, and G. C. Hadjipanayis, *J. Appl. Phys.*, **87**, 5308(2000).
10. W. Tang, Y. Zhang, and G. C. Hadjipanayis, *Appl. Phys. Letter.*, **77**, 421(2001).
11. J. F. Liu, Y. Ding, Y. Zhang, D. Dimitar, F. Zhang, and G. C. Hadjipanayis, *J. Appl. Phys.*, **85**, 5660(1999).
12. L. Cataldo, A. Lefevre, F. Ducret, M.-Th. Cohen-Adad, C. Allibert, and N. Valignat, *J. Alloys Compd.*, **241**,216(1996).
13. M. Katter, J. Weber, W, Assmus, P. Schrey, and W. Rodewald, *IEEE Trans. Magn.* **32**, 4815(1996).
14. M. V. Satyanarayana, H. Fujii, and E. Wallace, *J. Appl. Phys.* **53**, 2374(1982).
15. W. Tang, Y. Zhang, and G. C. Hadjipanayis, *J. Magn. Magn. Mater.* **212**, 138(2000).
16. W. Tang, Y. Zhang, and G. C. Hadjipanayis, *J. Appl. Phys.*, **87**, 399(2000).
17. S. Liu and E. P. Hoffman, *IEEE Trans. Magn.*, **32**, 5091(1996).
18. C. Chen, M. S. Walmer, and M. H. Walmer, *J. Appl. Phys.*, **83**, 6706(1998).
19. J. F. Liu, Y. Ding, and G. C. Hadjipanayis, *J. Appl. Phys.*,**85**, 1670(1999).
20. H. Kronmuller, in *Magnetic hysteresis in novel magnetic materials*, NATO ASI Series, 338(1997).
21. Y. Zhang, W. Tang, and G. C. Hadjipanayis, *Proceedings of the sixteenth international workshop on rare earth magnets.* pp167-177, Sept. 14, 2000, Sendai, Japan.
22. B. Barbara and M. Uehara, *IEEE Trans. Magn.*, **12**, 997(1976).
23. A. V. Deryagin, *J. Physique*, **40**, 165(1979).
24. A. S. Ermolenko, *IEEE Trans. Magn.*, **12**, 992(1976).
25. J. D. Livingston, *J. Appl. Phys.*, **46**, 5259(1975).